Open access • Journal Article • DOI:10.1109/3.157

Quantum box fabrication tolerance and size limits in semiconductors and their effect on optical gain — Source link

Kerry J. Vahala

Institutions: California Institute of Technology

Published on: 01 Mar 1988 - IEEE Journal of Quantum Electronics (IEEE)

Topics: Quantum optics, Quantum number, Quantum well and Stimulated emission

Quantum Box Fabrication Tolerance and Size Limits in Semiconductors and Their Effect on Optical Gain

KERRY J. VAHALA, MEMBER, IEEE

Abstract—**Lower and upper limits on size are established for quantum boxes. The lower limit is shown to result from a critical size below which bound electronic states no longer exist. This critical size is different for electrons and holes. The optical gain of arrays of quantum boxes is computed taking into account the inhomogenous broadening of the gain spectrum resulting from fabricational variations in quantum box size and shape. The dependence of maximum possible gain on an rms quantum box roughness amplitude is determined. For high gain operation a medium composed of quantum boxes does not offer significant advantages over a conventional bulk semiconductor unless quantum box fabricational tolerances are tightly controlled. For low gain operation, however, arrays of quantum boxes may offer the unique advantage of optical transparency at zero excitation. This property does not require excellent fabricational control and may make possible ultralow threshold semiconductor lasers and low noise optical amplifiers.**

INTRODUCTION

DIRECT write lithography technology is now capable of fabricating structures having nanometer scale feature sizes. If combined with epitaxially-grown quantum well material in systems like GaAs(AlGaAs) or InGaAsP(InP) structures exhibiting quantum size effects in two or three dimensions can be contemplated. Quantum wires and quantum boxes are examples of such structures [1]–[4].

It has been proposed that arrays of quantum wires or quantum boxes might be used as the active layer of a semiconductor laser [5]. In these devices the quantum wires or quantum boxes, composed of a low band-gap material like GaAs, would be imbedded in a higher band-gap material like AlGaAs (see Fig. 1). Theoretical studies indicate the potential advantages of these structures are reduced threshold current densities [5], [6], improved phase noise characteristics (i.e., reduced field spectrum linewidths) [7], [8], and improved T_o's [5]. Some of these effects have been observed by simulating quantum boxes and quantum wires using high magnetic fields [7], [8].

These improvements result from the narrower optical gain spectrum provided by these structures. In essence, the importance of Fermi statistics in shaping the gain profile is reduced as confinement is increased in one or more dimensions. To clarify this point consider a simple model of the optical gain spectrum. This model assumes that rigorous k-selection rules hold and ignors any homogenous broadening associated with the individual optical transitions. The optical gain spectrum is then directly proportional to the density of states function $D_d(E)$ where d is the system dimension. $D_d(E)$ is illustrated in Fig. 2 for various dimensions d. A typical gain profile is also shown in each case as the dashed curve. The narrowing of the gain spectrum with increasing quantum confinement (decreasing d) is apparent. Subsequent improvements in the static and dynamic properties of the laser are also obvious. Threshold current, for example, must decrease as the spectrum narrows (all other factors remaining the same) since to achieve threshold fewer carriers are wasted in regions of spectral space that do not contribute to lasing action. These effects have been experimentally verified in quantum well semiconductor lasers where lower threshold currents and superior dynamic performance as compared to the conventional device have been demonstrated [9], [10].

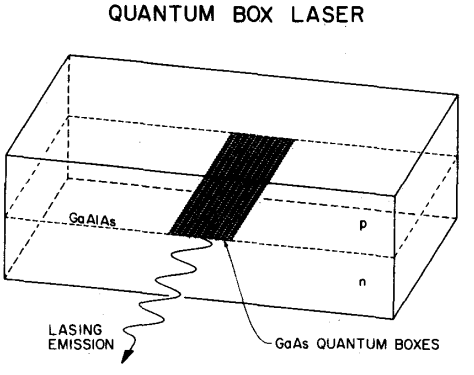

Fig. 1. A quantum box semiconductor laser in the GaAs (AlGaAs) system. The quantum boxes are not drawn to scale.

The above model also shows that a quantum box active layer is the optimal choice to achieve maximum improvement in semiconductor laser performance. With a quantum box the gain spectrum broadening associated with the effective density of states is reduced to zero. This leaves

Manuscript received June 4, 1987; revised October 12, 1987. This work was supported in part by the National Science Foundation and by the U.S. Office of Naval Research.

The author is with the Department of Applied Physics, California Institute of Technology, Pasadena, CA 91125.

IEEE Log Number 8718527.

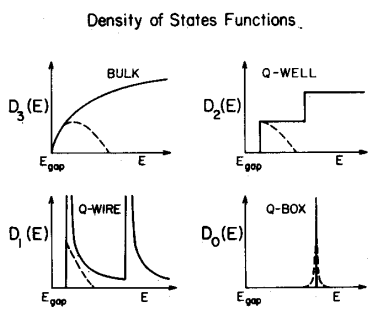

Fig. 2. The density of states function for zero-, one-, two-, and three-dimensional systems. The dashed curve indicates approximately the optical gain which results when the medium is inverted.

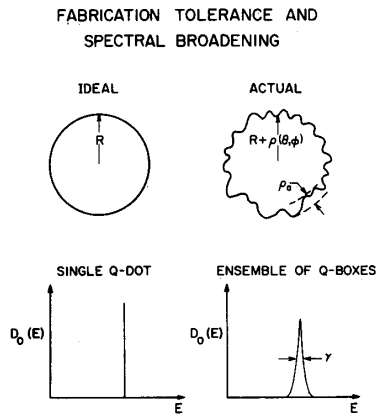

Fig. 3. The cross section of ideal and actual quantum boxes appears in the upper half of the figure. The boundary indicates the separation between low and high band-gap material. The roughness function and roughness amplitude are introduced to account for fabricational imperfections. In the lower half of the figure the density of states function for a single quantum box appears as a delta function. An ensemble of quantum boxes, however, is inhomogeneously broadened by random fluctuations in quantum box size and shape.

only the natural linewidth of the optical transition (homogeneous broadening). This paper will focus on the quantum boxes as a source of optical gain. It differs from previous treatments of this subject in that the practical problems and limitations affecting the optical gain attainable with an array of quantum boxes are addressed. There are a host of problems associated with fabricating quantum box active layers which we must assume to be surmountable. There remain, however, basic theoretical questions concerning the quantum box volumetric density required to furnish a given optical gain, the limitations imposed on quantum box size, and the tolerances which must be maintained during fabrication. Fabrication tolerance will be of central importance since it determines the degree to which the optical gain spectrum is inhomogeneously broadened (see Fig. 3). It may be the case that a quantum box laser is theoretically feasible, but highly unrealistic in terms of the required fabricational tolerances. For example, since two dimensions of the quantum box are defined by a combination of beam writing and subsequent processing, it would be highly unrealistic to assume that these dimensions could be held to the same tolerance that can be achieved in the other direction by epitaxial means (e.g., held to a monolayer or less with molecular beam epitaxy).

In this paper we attempt to answer these questions. We will calculate the optical gain achievable with a given density of quantum boxes and study the effect of fabrication tolerance on the optical gain. In addition to studying optical gain we will address the issue of upper and lower limits on quantum box size, establishing allowable ranges and introducing a critical quantum box radius below which there are no bound electronic states in a quantum box. Two regimes of quantum box size will be discussed below. The behavior of optical gain with pumping will be seen to depend on the particular quantum box regime selected.

Quantum Box Size Limitations

It is necessary to establish what the characteristic sizes of quantum boxes must be and to determine if there are limits imposed on the range of allowable sizes. The model of quantum boxes employed here will be based on the effective mass approximation and will assume the carriers in the box behave as particles in a spherical well. The spherical well potential, unlike the three-dimensional square well potential employed elsewhere is separable and thus lends itself to simplified analytical solutions. Electronic states in these structures are given by the kets $| k, j, m \rangle_n$ where j is the quantum number of total angular momentum, m is the z-component of angular momentum, k is a quantum number associated with radial motion and the subscript n is an energy band index. An optical dipole transition from the conduction band to the valence band conserves j and m in the single electron approximation. This rule differs from its free-space counterpart because the j and m employed here refer to envelope functions in the effective mass approximation. k is also conserved provided that the wave function does not extend significantly outside of the well. A transition from the lowest energy eigenstate of the conduction band will therefore be to the highest energy eigenstate in one of the respective valence bands. This rule will be assumed to hold rigorously throughout this analysis.

The two lowest energy eigenstates occur for $j = 1/2$, $m = \pm 1/2$. These correspond to the two spin states having zero orbital angular momentum. The radial quantum number for these states obeys a particularly simple eigenvalue equation which upon soluton of the Schrodinger equation in spherical coordinates is easily shown to be [11]

$$\sqrt{\frac{2m_e V_o}{\hbar^2} - k^2} = -k \cot(kR) \tag{1}$$

where m_e is the effective mass, V_o is the depth of the well, and R is the radius of the quantum box. The eigenenergy

E is related to k through the familiar expression,

$$E = \frac{\hbar^2 k^2}{2m_e}. \tag{2}$$

Equations (1) and (2) are similar to the eigenvalue equations for a one-dimensional potential well of width w and depth V_o if we make the correspondence $R \rightarrow w$. In fact, the eigenvalues of (1) correspond to the odd parity solutions in the one-dimensional well. Consequently, whereas the one-dimensional problem has a bound state for all w (i.e., the lowest energy even parity solution), there exists a critical radius R_c in the three-dimensional problem below which there are no bound states. For the spherical well this critical radius is given by

$$R_c = \frac{\pi}{2}\sqrt{\frac{\hbar^2}{2m_e V_o}}. \tag{3}$$

Three-dimensional wells of arbitrary shapes should also have such a critical size.[1] This fact seems to have gone unnoticed thus far in the study of quantum boxes. It has important consequences, one of which is illustrated in Fig. 4. There, (3) has been used to plot the critical quantum box diameter against the energy-gap difference between GaAs and AlGaAs. We have assumed effective masses of $0.067m_o$ for electrons and $0.47\ m_o$ for heavy holes in GaAs with m_o the free electronic mass. Furthermore, a 60–40 percent apportioning of the band-gap offset energy is assumed. Note that because of the large difference in the electron and hole effective masses there is a range of diameters for which there remain bound holes, but no bound electrons.

R_c for the electrons sets a lower limit on quantum box size. The upper limit is set by the need to create a "discrete" state space in at least one of the energy bands. A state space will appear discrete at a given temperature T if the energy spacing between states is larger than $k_B T$ (26 meV at room temperature). In a quantum box laser it is actually better to have the energy spacing still larger, since ideally only the two lowest energy states in a given band should contribute to lasing. As already noted, in the conduction band the lowest energy eigenstates are states of zero orbital angular momentum (i.e., $l = 0$). The next highest energy eigenstates, however, occur for $l = 1$. For the infinite potential well their energy separation from the lowest energy states is given by the expression

$$\Delta E_{1,0} \simeq 10.3\,\frac{\hbar^2}{2m_e R^2}. \tag{4}$$

For conduction band electrons in GaAs if $\Delta E_{1,0} = 3k_B T_{\text{room}}$ then $R = 87$ Å (i.e., a quantum box diameter d of 174 Å). At this energy separation the sixfold degenerate $l = 1$ states will have an electron Fermi occupancy of 0.047 when the Fermi level resides at the energy of the two lowest energy states. Consequently, for practical considerations involving computation of threshold gain, etc., the conduction band in a structure this small can be treated as one doubly-degenerate energy level.

[1]The existence of a critical size for quantum boxes of arbitrary shapes can be proven within the limits of the first-order perturbation approach used to derive (12). To see this consider an irregularly-shaped quantum box. The largest sphere that fits inside the box and the smallest sphere that contains the box can then be used to set upper and lower bounds on the quantum box eigenenergy. A critical size associated with each sphere then proves the existence of a critical size for the irregularly-shaped box.

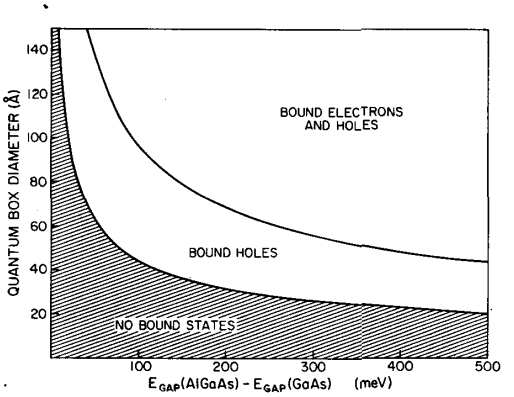

Fig. 4. The curves give critical quantum box diameters for electrons and holes at a given energy-gap difference between GaAs and AlGaAs. In the upper region bound states exist for both electrons and holes; in the intermediate region only bound hole states exist; and in the cross hatched region there are no bound states.

At this same diameter, however, the heavy hole system will remain a quasi-continuum owing to the heavy hole effective mass. This range of sizes will be referred to as the large quantum box regime. To achieve a discrete spectrum of states in both the conduction and valence bands the quantum box size must be reduced still further to what we call the small quantum box regime. For the purposes of demonstration we will neglect problems associated with valence band mixing effects and consider only the heavy hole band. To achieve a $\Delta E_{1,0} = 3k_B T_{\text{room}}$ for the heavy hole band in GaAs would require a quantum box diameter of 66 Å. If we tolerate an increased occupancy of lower energy hole states by reducing $\Delta E_{1,0}$ to $\Delta E_{1,0} = k_B T_{\text{room}}$ then a diameter of 114 Å is possible. In view of Fig. 4 it is clear that selection of such small diameters must be accompanied by an adequately deep well to guarantee the existence of bound electron states. The results of this section are summarized in Fig. 5. In particular, the small and large quantum box regimes are given at several temperatures for the material systems GaAs(AlGaAs) and GaInAs(InP). The latter system has been chosen because of its very light electronic effective mass ($0.04m_o$).

There are important differences between active layers composed of large quantum boxes and small quantum boxes. These will be addressed below.

Fabrication Tolerance and the Gain Spectrum

A quantum box semiconductor laser can be viewed as a gas laser in which the atoms are likened to the quantum boxes. The overall gain spectrum produced by this gas is broadened both homogeneously by the natural linewidth

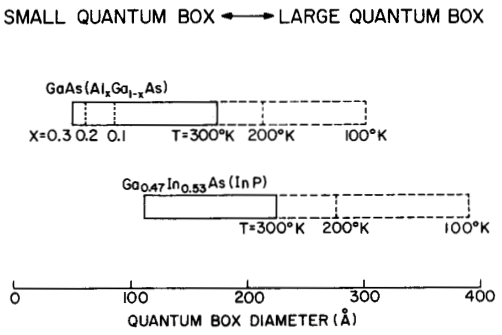

Fig. 5. The allowable ranges of quantum box size for two material systems. The lower limit is determined by the critical diameter below which there exist no bound electrons in the quantum box. The upper limit is set by the requirement that the quantum boxes exhibit measurably discrete spectra at a given temperature.

of a single transition in a given box and inhomogeneously by fabricational variations in the quantum box sizes. There is even the equivalent of pressure broadening in this system, since when the quantum box density becomes too large the state space broadens as a result of interaction between electrons in different quantum boxes. In this section the gain spectrum resulting from a given volumetric density of quantum boxes will be calculated.

The optical transition from conduction band state to valence band state in each quantum box is assumed to be homogeneously broadened according to a broadening function $g(E)$. In addition we must account for variations in transition energy resulting from the varying sizes of the quantum boxes. This produces an inhomogeneous broadening of the gain spectrum which we describe using a distribution function $D(E)$ (in effect, a density of states function) that is related to the distribution of quantum box sizes. The gain coefficient per unit time at frequency ω is related to these functions through the following expression [12]:

$$G(N, \omega) = 2 \int dE D(E - E_o)\, g(\hbar\omega - E) \cdot |M|^2 (f_c(N, E) - f_v(N, E)) \quad (5)$$

where E_o is the average transition energy, M is the matrix element for a quantum box transition, N is the carrier density, and $f_c(f_v)$ is the Fermi factor for the conduction (valence) band. A typical quantum box active layer will be composed of several hundred thousand quantum boxes. It is therefore reasonable to assume that $D(E)$ is a Gaussian distribution function of the form

$$D(E) = \frac{2\eta}{\gamma\sqrt{2\pi}} \exp\left(-\frac{1}{2}\left(\frac{E}{\gamma}\right)^2\right) \quad (6)$$

where η is the number of quantum boxes per unit volume (note: this quantity can have a spatial dependence) and where the normalization factor for $D(E)$ includes a factor of two to account for spin degeneracy.

The quantity γ gives a measure of the inhomogeneous broadening resulting from the variations in quantum box sizes (see Fig. 3). It is important to relate this quantity to actual statistical variations in quantum box size. Smearing of the optical transition energy will result primarily from variations of the lowest conduction band eigenenergy, because of the small conduction band effective mass. To simplify the calculation we therefore consider only variations in the conduction band eigenenergy that result from quantum box size variation (i.e., variations of valence state energies are ignored). Obviously, fluctuations in size and shape of a quantum box can take on a very complicated form as illustrated in Fig. 3. Therefore, to proceed consider first a simple variation δR of a perfectly spherical well. If the electron is tightly bound to the quantum box, as a result of either the well potential being deep or the quantum box being large, then it is adequate to approximate the well as infinitely deep. The lowest eigenenergy is then given by

$$E_c^\infty = \frac{\hbar^2\pi^2}{2m_e R^2} \quad (7)$$

and therefore the associated energy shift in the optical transition due to the variation δR is given by

$$\delta E = -2E_c^\infty \frac{\delta R}{R}. \quad (8)$$

In general, the potential cannot be treated as infinite. It is straightforward to show using (1) that a more general expression is given by

$$\delta E = -\xi E_c \frac{\delta R}{R} \quad (9)$$

where $\xi < 2$ approaches zero as the electron becomes more weakly bound.

To include the possibility of more complex shape and size variations we introduce an amplitude roughness function $\rho(\theta, \phi)$ which characterizes deviations from the ideal spherical well (see Fig. 3). We will assume that the actual well potential has the following form as a result of imperfections in the fabrication process:

$$V(r) = V_o U(r - R - \rho(\theta, \phi)) \quad (10)$$

where $U(r)$ is the Heaviside function. Upon application of first-order perturbation methods this yields the following expression for the resulting shift in the optical transition energy

$$\delta E = -V_o |\psi(R)|^2 R^2 \bar{\rho} \quad (11)$$

where $\bar{\rho}$ is the average of the roughness function $\rho(\theta, \phi)$ over 4π steradians and where $\psi(r)$ is the eigenfunction of the lowest energy conduction band state. In the limit of an infinite potential well (i.e., $V_o \to \infty$) it can be shown that this expression reduces to the following form:

$$\delta E = -2E_c^\infty \frac{\bar{\rho}}{R} \quad (12)$$

where E_c^∞ is given by (7). This is similar to (8) with $\bar{\rho}$ replacing δR. We will assume this relation also holds in

the finite well. Finally, it is helpful to relate $\bar{\rho}$ to a roughness amplitude ρ_a (see Fig. 3) by assuming a particular form for $\rho(\theta, \phi)$. For the purposes of demonstration we will assume that $\rho(\theta, \phi) = \rho_a \cos^2(a\theta) \cos^2(b\phi)$. For a and b large enough we obtain $\bar{\rho} = \rho_a/4$. Using this result and (9), the characteristic inhomogeneous linewidth, γ, can be expressed as

$$\gamma^2 = \langle \delta E^2 \rangle_e = \left(\frac{\xi E_c}{4R}\right)^2 \langle \rho_a^2 \rangle_e = \left(\frac{\xi E_c}{4R}\right)^2 \theta^2 \quad (13)$$

where $\langle\ \rangle_e$ indicates an average over the ensemble of quantum boxes and where $\theta^2 \equiv \langle \rho_a^2 \rangle_e$. That is, θ is an rms roughness amplitude for the ensemble of quantum boxes.

To simplify (5) we will assume that the homogeneous broadening function $g(E)$ is also a Gaussian of the following form:

$$g(E) = \frac{\hbar}{\delta}\sqrt{\frac{\pi}{2}} \exp\left(-\frac{1}{2}\left(\frac{E}{\delta}\right)^2\right). \quad (14)$$

The normalization here is chosen so as to recover Fermi's Golden Rule in (5) in the limit $\delta \to 0$. Using this form, the gain spectrum is given by

$$G(N, \omega) = \frac{4\eta |M|^2 \hbar}{\sqrt{2\pi}\sqrt{\gamma^2 + \delta^2}} \left(f_c(N, E_o) - f_v(N, E_o)\right) \exp\left(-\frac{(\hbar\omega - E_o)^2}{2(\gamma^2 + \delta^2)}\right) \quad (15)$$

where we have assumed both the matrix element and the quasi-Fermi factors are approximately constant over the width of the quantum box gain spectrum. This expression will now be studied for the two size regimes discussed in the previous section.

Small Quantum Boxes

Small quantum boxes have dimensions that cause the energy spectrum in the both the conduction and valence bands to be discrete. Equation (15) can be written in terms of the carrier density N by noting that $N = 2f_c\eta$ and by assuming that the quantum boxes are, on the average, quasi-neutral and undoped (i.e., $f_v = 1 - f_c$). Doing so yields

$$G_s = A_s(N - \eta) \exp\left(-\frac{(\hbar\omega - E_o)^2}{2(\gamma^2 + \delta^2)}\right) \quad (16)$$

$$A_s \equiv \frac{4|M|^2\hbar}{\sqrt{2\pi}\sqrt{\gamma^2 + \delta^2}}. \quad (17)$$

The gain is therefore linear in carrier density and abruptly saturates when all quantum boxes are filled (i.e., $N = 2\eta$). This is illustrated in Fig. 6 where G_s is plotted versus N. Transparency of the active layer occurs at the excitation level $N = \eta$.

It is also possible to calculate the optical gain when the quantum boxes have been doped. f_c or f_v will then be biased by the presence of donors or acceptors. In Fig. 6

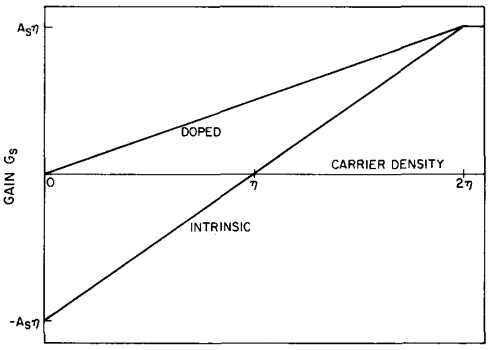

Fig. 6. Optical gain versus carrier density for an array of small quantum boxes with a density of η boxes per unit volume. For undoped quantum boxes the transparency excitation level occurs at a carrier density of η. For quantum boxes doped with two donors or acceptors per box the transparency excitation level is effectively zero. In both cases the optical gain saturates at a carrier density of 2η.

we have plotted the case of doping at a level of two donors or acceptors per quantum box. The differential gain A_s is reduced by doping. Notice, however, that a significant improvement in the transparency level has occured under doping. In fact, a nearly zero transparency level is expected. This result has important consequences to the design of lasers and optical amplifiers. For lasers it means there is no transparency penalty in achieving threshold. Extremely low threshold semiconductor lasers are therefore possible by simply reducing loss. In amplifiers, this eliminates the spontaneous noise associated with achieving transparency and hence reduces the overall amplifier noise at a given gain.

In Fig. 7 G_s as a function of carrier density has been plotted for the specific case of an array of quantum boxes having an average diameter $d = 100$ Å, center to center spacing 200 Å (i.e., $\eta = 1.25 \times 10^{17}$ cm^{-3}), and a fabricational tolerance $\theta = 20$ Å. Gain has been plotted in both temporal and spatial rate units. In performing this calculation we have used [12]

$$|M|^2 = \frac{E_o}{2\epsilon\hbar^2}|\mu|^2 \quad (18)$$

where ϵ is the dielectric constant of the material and μ is the component of the dipole matrix element in the direction of the electric field vector. In accordance with the results contained in [6], $|\mu|/q = 4$ Å, corresponding to the value in bulk GaAs, has been employed here. In addition $|\mu|^2$ has no field polarization dependence owing to the spherical symmetry of these lowest energy box states.

Large Quantum Boxes

A large quantum box falls at the other end of the range indicated in Fig. 5. It has a conduction band energy spectrum that is discrete, but its valence band remains a quasi-continuum. This makes it more difficult to invert the quantum box to achieve optical gain, since a large number of holes must be added to the structure to produce an ap-

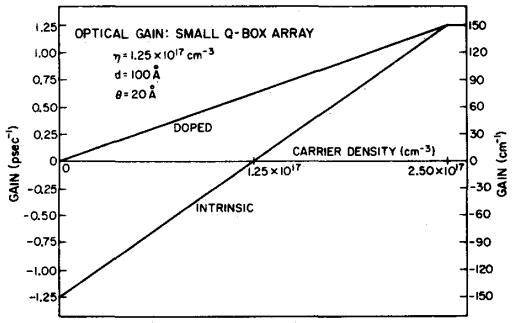

Fig. 7. Optical gain plotted versus carrier density for an array of small GaAs quantum boxes with average diameter d, density of boxes η, and rms roughness amplitude θ as indicated.

preciable hole occupancy in the highest energy state in the valence band. By quasi-neutrality these holes must be balanced by an equal number of electrons. The net effect is thus to increase the required threshold carrier density. To see this consider an undoped quantum box of diameter $d = 200$ Å. Suppose that this structure is quasi-neutral and contains a single electron and a single hole. Upon intraband thermalization the electron will occupy the lowest energy level of the conduction band. The hole occupancy, however, is smeared out over a larger number of valence band states owing to the narrow energy spacing of the heavy hole states.

The occupancy f_v at a given energy is related to the hole occupancy f_h by the expression $f_v = 1 - f_h$. In Table I f_v has been tabulated for various numbers of holes in this quantum box. The equivalent hole density is also given. The heavy hole effective mass in GaAs has been used for this calculation and we have assumed the hole state space to be a quasi-continuum. The optical gain of this structure will be proportional to $f_c - f_v$, the difference in electronic occupancies between the lowest energy conduction band state and the highest energy valence band state. Ideally, to achieve maximum gain we would like $f_c = 1$ and $f_v = 0$. For the present case of one electron and one hole in the quantum box, however, $f_c = 1$ and $f_v = 0.97$, resulting in a greatly-reduced optical gain. For this size quantum box the large effective mass of the heavy holes therefore undermines the potential advantages offered by the structure. To circumvent this problem the quantum boxes could be p-doped to bias f_v towards zero.

The optical gain of an array of large quantum boxes can also be expressed in terms of the injected carrier density N by using $N = 2\eta f_c$ and by treating f_v as a fixed quantity dependent upon the p-doping level. Using (15) we find

$$G_L = A_L(N - 2\eta f_v) \exp\left(-\frac{(\hbar\omega - E_o)^2}{2(\gamma^2 + \delta^2)}\right) \quad (19)$$

$$A_L \equiv \frac{2|M|^2\hbar}{\sqrt{2\pi}\sqrt{\gamma^2 + \delta^2}}. \quad (20)$$

This function, like G_s, is linear in carrier density and saturates when $N = 2\eta$. It is plotted in Fig. 8 for the various

TABLE I
HOLE VOLUMETRIC DENSITY AND ELECTRONIC OCCUPANCY[a]

Hole No.	Hole Density (cm^{-3})	f_v
1	2.4×10^{17}	0.97
[a] 5	1.2×10^{18}	0.86
[b] 25	5.6×10^{18}	0.50
[c] 50	1.2×10^{19}	0.29

[a]Hole volumetric density and electronic occupancy (i.e., $f_v = 1 - f_h$) for various numbers of holes in a 200 Å diameter GaAs quantum box. The letters a, b, c refer to Figs. 8 and 9.

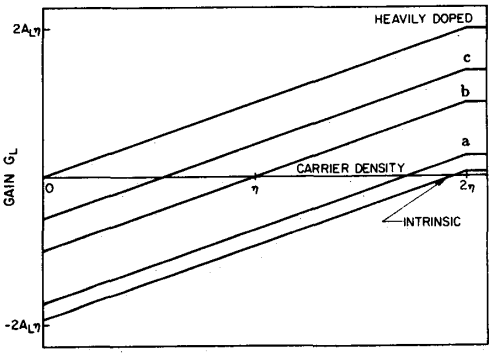

Fig. 8. Optical gain versus carrier density for an array of large quantum boxes at various levels of p-doping (a, b, c correspond to f_v given in Table I). The reduction in transparency excitation level with increased p-doping is apparent.

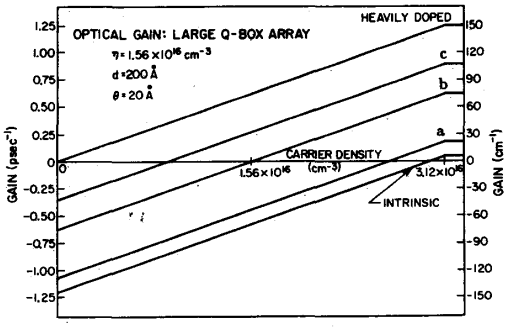

Fig. 9. Optical gain versus carrier density for an array of large GaAs quantum boxes with density of boxes η, box diameter d, and rms roughness amplitude θ as indicated. The different curves correspond to different p-doping levels (a, b, c correspond to the levels given in Table I).

p-doping levels given in Table I. The effect of p-doping on the transparency level is apparent. In Fig. 9 a specific case is plotted in which the array contains quantum boxes having a diameter $d = 200$ Å, center to center spacing of 400 Å (i.e., $\eta = 1.56 \times 10^{16}$ cm^{-3}), and a fabricational tolerance $\theta = 20$ Å. It should be noted that the introduction of heavy p-doping will produce strong Coulomb effects which will in turn alter the electronic state-space of the quantum box [13]. Such heavily-doped structures would become a variation of the so-called superatom [14]. These effects will not be addressed here.

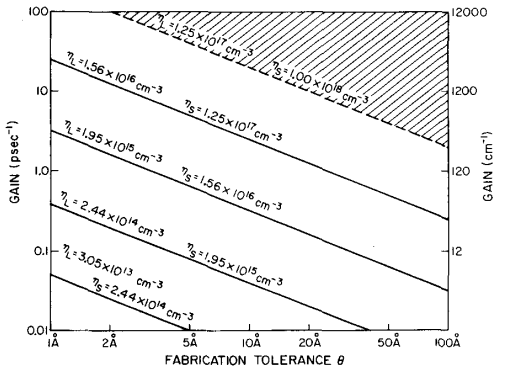

Fig. 10. Maximum possible optical gain versus fabrication tolerance (given as the rms roughness θ) for arrays of quantum boxes of various densities. Large quantum boxes (density η_L) have an average diameter of 200 Å and small quantum boxes (density η_S) have an average diameter of 100 Å. The cross hatched region is beyond the geometrical packing limit of the quantum boxes.

Maximum Possible Gain

For the purposes of determining whether lasing threshold is possible it is necessary to estimate the maximum optical gain possible with a given density of quantum boxes having a given fabricational tolerance. For the large quantum box array the maximum possible gain is $2A_L\eta$ (assuming heavy p-doping) and for the small quantum box array maximum possible gain is $A_S\eta$. In Fig. 10 we show how these quantities vary with fabricational tolerance θ for 100 Å small quantum boxes and 200 Å large quantum boxes. In general, large quantum boxes are less susceptible to fabricational induced smearing of the gain spectrum [see (13)]. As a result higher gains for given quantum box densities are possible as compared to the small quantum box case. The cross hatched region of the figure is forbidden. It corresponds to densities beyond those possible with the assumed quantum box diameters (note: cubic packing is assumed). The homogenous linewidth has been neglected in making these plots. Obviously, however, the presence of a finite homogenous linewidth will cause these curves to flatten as θ decreases. For the purpose of comparison θ = 10 Å corresponds to an energy broadening of 2.8 meV for the large quantum boxes and 22.6 meV for the small quantum boxes.

Conclusion

Arrays of quantum boxes may one day be employed as sources of optical gain in lasers or amplifiers. We have established size limitations on the quantum boxes in these arrays and have studied the dependence of optical gain on quantum box fabricational tolerance. The lower limit on quantum box size is set by the disappearance of bound electronic states at a critical diameter. We have calculated this critical diameter for the spherical quantum box and have shown that it differs for electrons and holes owing to the difference in their effective masses. The upper limit on quantum box size is set by the need to generate a discrete spectrum of states in one or both of the principal energy bands. When both the conduction band and valence band spectra are discrete, the quantum box is in the small regime. When only the conduction band spectrum is discrete the quantum box is in the large regime. The optical properties of quantum box arrays is regime dependent. Each regime has its own advantages and disadvantages. For example, it would appear unlikely that an array of large quantum boxes would provide the necessary gain for lasing action (even under high excitation) unless it is heavily p-doped. An array of small quantum boxes, on the other hand, can provide gain without being doped. Large quantum boxes, however, are easier to fabricate and once p-doped should attain higher optical gains for a given quantum box density at a given excitation level. This is a direct result of their gain spectra being less sensitive to fabricational induced broadening.

To compare quantum box arrays and bulk semiconductor material in terms of their optical gain at a given excitation level, it is useful to distinguish between the cases of high and low gain. To achieve the very high gains typical of a conventional semiconductor laser (e.g., tens of cm^{-1}), arrays of quantum boxes do not offer significant advantages unless there is very good control of fabricational tolerance. For example, Fig. 9 indicates improvements in threshold carrier density exceeding two orders of magnitude (bulk carrier densities of 3×10^{18} cm^{-3} are typical for an optical gain of 50 cm^{-1}) provided the rms roughness amplitude is held to 20 Å on an array of 200 Å diameter quantum boxes. Since 200 Å diameter quantum boxes have not yet been fabricated it is impossible to assign a difficulty factor to this specification. It most probably exceeds the state-of-the-art in direct-write lithography, however.

For low optical gains, however, a quantum box medium may offer a unique advantage that does not require extremely good fabricational control. This is a nearly-zero transparency level made possible by p-doping the quantum boxes. This property may make possible very low threshold semiconductor lasers provided that cavity losses are substantially reduced. It may also lead to optical amplifiers with improved noise characteristics. We will investigate these applications elsewhere.

References

[1] P. M. Petroff, A. C. Gossard, R. A. Logan, and W. Wiegmann, "Toward quantum well wires: fabrication and optical properties," *Appl. Phys. Lett.*, vol. 41, pp. 635-638, 1982.

[2] K. Kash, A. Scherer, J. M. Worlock, H. G. Craighead, and M. C. Tamargo, "Optical spectroscopy of ultrasmall structures etched from quantum wells," *Appl. Phys. Lett.*, vol. 49, pp. 1043-1045, 1986.

[3] J. Cibert, P. M. Petroff, G. J. Dolan, M. B. Panish, and S. N. G. Chu, "Optically detected carrier confinement to one and zero dimension in GaAs quantum well wires and boxes," *Appl. Phys. Lett.*, vol. 49, pp. 1275-1277, 1986.

[4] H. Temkin, G. J. Dolan, M. B. Panish, and S. N. G. Chu, "Low temperature photoluminescence from InGaAs/InP quantum wires and boxes," *Appl. Phys. Lett.*, vol. 50, pp. 413-415, 1987.

[5] Y. Arakawa and H. Sakaki, "Multidimensional quantum well laser and temperature dependence of its threshold current," *Appl. Phys. Lett.*, vol. 24, pp. 195-197, 1982.

[6] M. Asada, Y. Miyamoto, and Y. Suematsu, "Gain and the threshold of three-dimensional quantum-box lasers," *IEEE J. Quantum Electron.*, vol. QE-22, pp. 1915-1921, Sept. 1986.

[7] Y. Arakawa, K. Vahala, and A. Yariv, "Dynamic and spectral properties of semiconductor lasers with quantum-well and quantum-wire effects," *Surf. Sci.*, vol. 174, pp. 155-162, 1986.
[8] K. Vahala, Y. Arakawa, and A. Yariv, "Reduction of the field spectrum linewidth of a multiple quantum well laser in a high magnetic field-spectral properties of quantum dot lasers," *Appl. Phys. Lett.*, vol. 50, pp. 365-367, 1987.
[9] W. T. Tsang, Extremely low threshold (AlGa)As graded-index waveguide separate confinement heterostructure lasers grown by molecular beam epitaxy," *Appl. Phys. Lett.*, vol. 40, pp. 217-219, 1982.
[10] A. Yariv, "Quantum well lasers and optoelectronics," in *Proc. CLEO'87*, paper WC1.
[11] A. Messiah, *Quantum Mechanics*, vol. 1. New York: Wiley, 1976.
[12] K. Vahala and A. Yariv, "Application of an electronic wave-packet formalism to operator equations of motion for semiconductor lasers," *Phys. Rev. A*, vol. 32, pp. 345-356, 1985.
[13] L. Brus, "Zero-dimensional "excitons" in semiconductor clusters," *IEEE J. Quantum Electron.*, vol. QE-22, pp. 1903-1914, 1986.
[14] T. Inoshita, S. Ohnishi, and A. Oshiyama, "Electronic structure of the superatom: A quasiatomic system based on a semiconductor heterostructure," *Phys. Rev. Lett.*, vol. 57, pp. 2560-2563, 1986.

Kerry J. Vahala (S'82-M'84-S'84-M'85), photograph and biography not available at the time of publication.